

# Exploiting Singular Configurations for Controllable, Low-Power Friction Enhancement on Unmanned Ground Vehicles

Adam Foris<sup>1</sup>, Nolan Wagener<sup>2</sup>, Byron Boots<sup>3</sup>, and Anirban Mazumdar<sup>1</sup>

**Abstract**—This paper describes the design, validation, and performance of a new type of adaptive wheel morphology for unmanned ground vehicles. Our adaptive wheel morphology uses a spiral cam to create a system that enables controllable deployment of high friction surfaces. The overall design is modular, battery powered, and can be mounted directly to the wheels of a vehicle without additional wiring. The use of a tailored cam profile exploits a singular configuration to minimize power consumption when deployed and protects the actuator from external forces. Component-level experiments demonstrate that friction on ice and grass can be increased by up to 170%. Two prototypes were installed on a 1:5 scale, radio-controlled rally car and tested. The devices were able to controllably deploy, increase friction, and greatly improve acceleration capacity on a slippery, synthetic ice surface.

**Index Terms**—Mechanism Design, Wheeled Robots

## I. INTRODUCTION

WHILE autonomous mobility on paved roads has seen major advancements, off-road and diverse terrain remains challenging. Varying conditions are particularly challenging for autonomous systems because these systems often lack the intuition, perception, and adaptive capacity of human drivers. Human operators not only adapt their driving to modulate friction [1], but they also physically modify their vehicles for different terrain. Specifically, humans can modulate the frictional performance of their vehicles by changing the tires or adding chains. This has proven highly effective, but autonomous systems cannot rely on a human expert to intervene every time the environment changes.

This work presents a new type of adaptive wheel intended for friction modulation. The core contributions of this work are the analysis, design, and validation of the spiral cam system. This unique approach enables modular attachment to

existing vehicles and low power consumption by exploiting a singular configuration. Additionally, this work demonstrates and quantifies the performance increase when this system is used on a slippery, ice-like surface.

Currently, many methods rely on static designs that are optimized for specific terrain (e.g., asphalt, off-road, or snow) [2]. Since static systems do not modulate behavior, they can be simple and robust to physical damage. Winter tires with friction-enhancing studs are a good example of static systems [3]. However, these systems cannot be easily changed and suffer from sub-optimal performance when used on terrain that differs from the design terrain [4]. As a result, there exists a growing research focus on adaptive ground locomotion systems that can adjust properties.

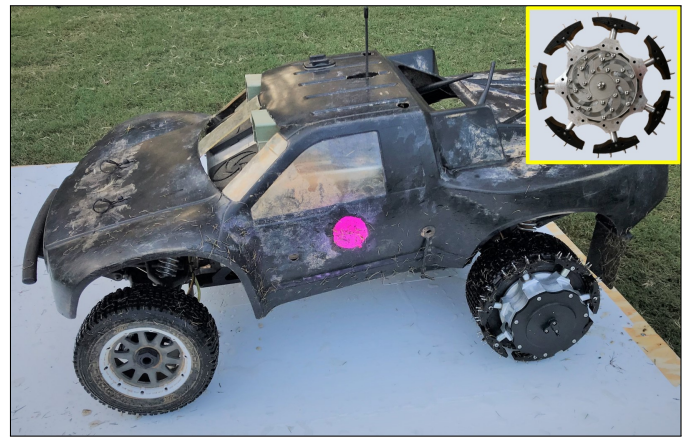


Fig. 1. Traction augmentation system installed on the rear wheels of a Georgia Tech AutoRally vehicle [5].

Adaptive wheel development is a rich and diverse research area. Existing methods fall into two broad categories: passive and active. Passive methods utilize mechanical intelligence to deploy or modify properties based on physical interaction between vehicle and terrain. These systems are appealing because they do not require power or communication. Power and communication can add considerable complexity. Examples of passive methods include spring-loaded variable diameter wheels [6], [7], wheels that can transform into legs [8], and footpads that deploy when slip occurs [9]. Similarly, spring-loaded microspines have shown great promise in this area and have enabled legged locomotion on vertical surfaces [10], [11]. Passive systems can be highly effective but cannot be easily modulated or controlled. As a result, they can be vulnerable

Manuscript received: September, 10, 2019; Revised December, 17, 2019; Accepted January, 25, 2020.

This paper was recommended for publication by Editor Paolo Rocco upon evaluation of the Associate Editor and Reviewers' comments. This work was supported by the Georgia Tech Institute for Robotics and Intelligent Machines and the NSF Graduate Research Fellowship Program (NSF 2015207631).

<sup>1</sup>A. Foris and A. Mazumdar are with the Woodruff School of Mechanical Engineering, Georgia Institute of Technology, Atlanta, GA 30332, USA foris.adam@gatech.edu, anirban.mazumdar@me.gatech.edu

<sup>2</sup>N. Wagener is with the Institute for Robotics and Intelligent Machines, Georgia Institute of Technology, Atlanta, GA 30332, USA nolan.wagener@gatech.edu

<sup>3</sup>B. Boots is with the Paul G. Allen School of Computer Science & Engineering, University of Washington, Seattle, WA 98195, USA bboots@cs.washington.edu

Digital Object Identifier (DOI): see top of this page.

to damage or wear.

Active systems, on the other hand, require energy input to change configuration. Such systems are generally difficult to deploy on wheels due to the rotation. However, recent works have shown how wheel diameter can be modulated using flexible structures [12], [13] or linkages [14], [15]. Active systems can also provide the capacity to controllably transition between wheeled and legged locomotion [16], [17], wheeled and tracked motion [18], [19], or between legged, pseudo-wheeled, and tracked [20]. Active systems offer the most flexibility, but may be limited by their complexity, fragility, and power requirements. To be effective solutions for autonomous off-road driving, active systems must dramatically modulate friction, draw little power, have minimal complexity, and be physically robust.

In this work, we propose a novel, spiral cam-based system that can be easily added to a wheel via a simple mounting component, isolates the drive motor from shocks, and only consumes actuation power when changing configuration. This design, highlighted in Fig. 1, utilizes a spiral profile that provides variable gearing and exploits a singular configuration. This system can be controlled wirelessly, requires few sensors, and helps minimize power consumption.

We begin by outlining a set of functional requirements for friction-adaptive wheels. We then describe our new spiral-cam approach and provide mathematical analysis for its spiral shape and variable transmission ratio. Based on this analysis, a physical prototype is constructed and characterized on the bench level. The results validate the intended geometric properties and demonstrate how friction coefficients can be dramatically increased on a variety of terrain. Finally, we discuss how our system is incorporated into a Georgia Tech AutoRally vehicle [5] and demonstrate improved driving on a very low friction surface.

## II. FUNCTIONAL REQUIREMENTS

In this section, we describe the functional requirements for an adaptive wheel mechanism intended for an autonomous, off-road car, truck, or buggy. For the scope of this work, we focus on the Georgia Tech AutoRally vehicle, which is a 1:5 scale, rear-wheel drive RC truck with a loaded mass of 22 kilograms [5]. However, these requirements are intended to be broadly applicable. We seek designs that minimize additional mass, complexity, and power consumption, while also providing robustness to substantial loads.

- 1) **Controllable deployment:** The primary aim of the platform is to augment traction only when necessary. This means that the wheel morphology can be controlled by the central vehicle control system. This differs from reflexive designs that react quickly but without centralized control.
- 2) **High force actuation:** Since the system is required to be controllable, the actuation system must be capable of generating sufficient forces to deploy the mechanism. In our example, the largest forces occur when increasing the effective wheel diameter (in order to deploy spikes beyond the original tire diameter). This requires each

adaptive wheel to lift a fraction of the fully loaded vehicle's weight. For the Georgia Tech AutoRally vehicle, this is 55N per adaptive wheel.

- 3) **Modular unobtrusive form factor:** We seek systems that can be readily added to a range of vehicles. This means that the system can be easily mounted to the wheel without replacing parts of the brakes, suspension, or vehicle body. Therefore, the system should be compact, self-powered, and easily attached to the wheel.
- 4) **Low power consumption:** Since the system is compact and self-powered, it must have low power consumption. Since the system will largely exist in either the deployed or stowed configurations, the actuators should not be required to maintain either posture. Actuator power should only be used when changing the configuration of the mechanism.
- 5) **Robustness to external loads:** Off-road driving can induce large forces and accelerations, especially when the terrain differs widely. With controllable mechanisms, the actuator is frequently a failure mode. Thus, methods that protect the actuator can greatly enhance robustness.

Our review of existing literature failed to provide a solution that meets our requirements, especially for a scaled vehicle. A potential solution has been highlighted in mass media [21]. However, such reports do not provide details regarding functional requirements, electromechanical design, or technical performance. Perhaps the most relevant existing method is the ability to switch between wheeled and tracked locomotion [18], [19]. This system differs from our approach because it changes the mode of locomotion and is currently focused on large-scale vehicles.

In contrast to existing methods, our approach maintains the locomotion mode, utilizes a hub-mounted spiral cam for selective deployment, and exploits a singular configuration for energy efficiency and robustness. This system can be controllably actuated using a small electric motor, consumes minimal power when stowed or fully deployed, and is able to protect the actuator from harsh driving conditions.

## III. MECHANISM DESIGN

Our overall design framework is shown in Fig. 2. The design utilizes high friction surfaces to dramatically increase the coefficient of friction over standard rubber tires on slippery terrain such as wet grass and ice. To deploy these surfaces, a spiral cam mechanism converts rotational input motion to linear output motion. As a result, the high friction surfaces can be made to extend outward, thereby increasing friction and also slightly increasing the working diameter of the wheel. This system consists of two core subsystems: a set of high friction surfaces, and the spiral cam. We now describe each of these subsystems in detail.

### A. Terrain Gripper High Friction Surface

Friction enhancement for tires is currently achieved using specially formulated rubbers, tire geometries [22], studs or chains for driving on ice. However, these systems cannot be automatically deployed or stowed. While these systems

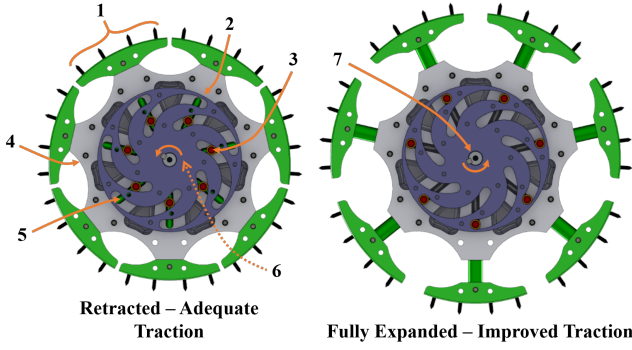


Fig. 2. Annotated mechanism with retracted and extended configurations: 1. Terrain gripper, 2. Spiral cam, 3. Guide pin, 4. Wheel mount, 5. Wheel mount linear pockets, 6. Cam-extending rotation direction, 7. Central drive shaft.

perform well on their target terrains, performance tends to be low and susceptibility to damage or wear increases on other surfaces such as asphalt. Deployable friction enhancing devices can help prevent this trade-off.

In this paper, we focus on enhancing friction on three candidate off-road surfaces: 1) ice, 2) grass, and 3) dry, packed dirt. The primary mechanisms influencing a tire’s grip on a surface are adhesion and deformation [23]. Viscoelasticity of the rubber causes distortion of the tire when forced into contact with surface asperities, thereby creating mechanical interference between tire and surface [24]. This distortion largely contributes to the tire’s holding force. The other important factor is the strength,  $\sigma$ , of materials in contact. For the ground-tire interaction to remain static, neither surface may shear away from its respective substrate. Combining these factors over all such discrete interactions yields a simple guiding relation for frictional holding force,  $F_h$ , as a function of perpendicular indentation area,  $A_i$ , as given in Eq. (1). Note that the frictional interface is assumed to be static and  $\sigma_s$  represents the lower of the two contacting material strengths.

$$F_h \propto \sum_{i=1}^n A_i \sigma_s \quad (1)$$

Based on Eq. (1), increased grip may be achieved through more indentations or increased cross sectional indentation area. For instance, a more compliant gripper material potentially increases the number of indentations *and* the indentation area. However, such a choice may not provide benefit for all conditions. In general, compliant materials have lower strength and longevity. Such an approach also neglects the fact that highly compliant contact can trap water in surface asperities, thus inhibiting indentation [25].

Our solution aims to increase indentation area on a variety of terrains (see Fig. 3). To puncture surfaces such as ice, cylindrical pins are sharpened to create spikes. An array of spikes is then assembled to create an enhanced friction surface. The configuration of such an array depends on the desired performance. Our approach draws a relatively equal balance between achievable indentation area, spike structural integrity, and anticipated wear performance. It features two identical rows of equally spaced spikes installed on a partial

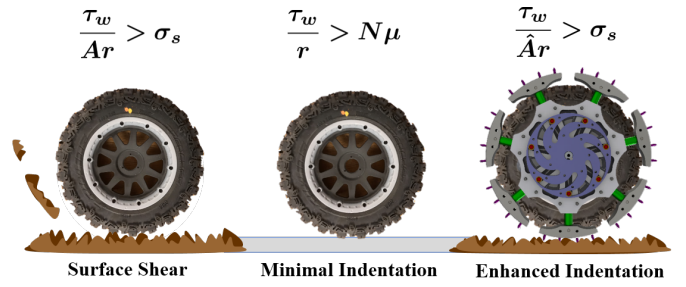


Fig. 3. Selection of a suitable terrain gripper relies primarily on its indentation capacity and the mechanical properties of the terrain. This figure presents three wheel-slip scenarios with corresponding slip conditions, where  $\tau_w$  is wheel torque,  $A$  indentation area,  $r$  wheel radius,  $\sigma_s$  terrain strength,  $\mu$  static friction coefficient,  $N$  normal force, and  $\hat{A}$  mechanism-enhanced indentation area.

arc. We refer to these arcs with spikes installed as “terrain grippers.” There are other configurations that optimize any given performance metric. For example, a staggered arrangement may minimize material accumulation on a gripper at the expense of structural integrity. The chosen configuration produces acceptable indentation on a wide variety of surfaces and is largely independent surface wetting.

### B. Expansion Mechanism (Spiral Cam)

We use a spiral cam to controllably deploy a set of terrain grippers. Since rotary, electromagnetic actuators are readily available, compact, and easy to control, we sought a mechanism that converts input rotary motion to linear output motions. Our methodology is shown in Fig. 2.

In Fig. 2, the “wheel mount” (gray) is connected directly to the wheel. For this discussion, we assume the wheel is temporarily stationary. The rotary input from a drive motor is converted to radial linear extension/retraction of each terrain gripper (green). From the initial, retracted state, motor torque rotates the spiral cam and its slots (purple) into contact with the guide pin (red) fixed to each terrain gripper. The resulting contact angle imposes outward motion relative to the wheel mount center. Linear pockets in the wheel mount further constrain motion of the guide pins such that the grippers, being fixed to guide pins, extend out radially relative to wheel mount center.

The input-output behavior of the spiral cam can be tuned based on speed, force, or packaging requirements. We analyze the input-output behavior by focusing on one cam slot. As Fig. 4 illustrates, the path of the cam slots is a circular arc of radius  $R$ . The cam slot arc’s center is offset from that of the input axis of rotation by displacements  $x_c$  and  $y_c$ . By offsetting the path center, an angle,  $\theta(\psi)$ , develops between the position vectors  $\vec{h}(\psi)$  and  $\vec{p}(\psi)$ . These vectors are shown in Fig. 4 and represent the vector connecting the cam slot and the input axis of rotation ( $\vec{h}(\psi)$ ) and the vector connecting the cam slot and the center of the cam slot arc ( $\vec{p}(\psi)$ ). Location along the path is defined by the path angle,  $\psi$ . We define the magnitudes of  $\vec{h}(\psi)$  and  $\vec{p}(\psi)$  as  $|\vec{h}|$  and  $|\vec{p}|$ , respectively.

$$\vec{h}(\psi) = \langle R \cos(\psi) + x_c, R \sin(\psi) + y_c \rangle \quad (2)$$

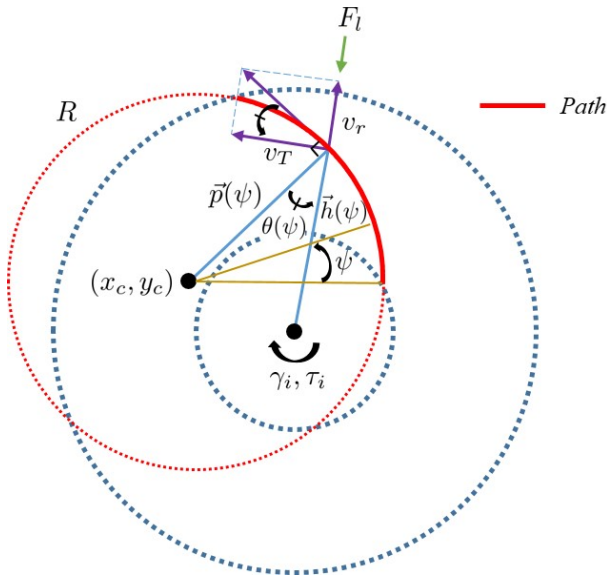


Fig. 4. Spiral cam geometric design framework.

$$\vec{p}(\psi) = \langle R \cos(\psi), R \sin(\psi) \rangle \quad (3)$$

$$\cos(\theta(\psi)) = \frac{\vec{h} \cdot \vec{p}}{|\vec{h}| |\vec{p}|} \implies \theta(\psi) = \cos^{-1} \left( \frac{\vec{h} \cdot \vec{p}}{|\vec{h}| R} \right) \quad (4)$$

The angle  $\theta(\psi)$  defines the kinematic relationship between the tangential cam slot velocity,  $v_T$ , and the output guide pin radial velocity,  $v_r$ . The relationship between  $v_T$  and the angular velocity of the cam,  $\dot{\gamma}$ , is shown in Eq. (5).

$$v_r = \dot{\gamma} |\vec{h}| \tan(\theta(\psi)) \quad (5)$$

Our system can be treated as a rotary-linear transmission with input-output ratio  $N$ . Note that our system has a variable transmission ratio that changes with configuration.

$$N = \frac{\dot{\gamma}}{v_r} = \frac{1}{|\vec{h}| \tan \theta(\psi)} \quad (6)$$

Energy losses in the mechanism are minimized by utilizing lubricated bushings and ball bearings on all moving parts in the mechanism. Assuming losses to be negligible, conservation of energy can be used in combination with Eq. (5) to determine the kinetic relationship between rotary input and linear output. Specifically, we seek the input torque,  $\tau_i$ , required to overcome the local linear load  $F_l$ .

$$\tau_i = \frac{v_r F_l}{\dot{\gamma}} = F_l |\vec{h}| \tan(\theta(\psi)) = \frac{F_l}{N} \quad (7)$$

For our application, we impose two core requirements on the spiral cam geometry. First, we desire relatively rapid deployment such that the transmission ratio,  $N$ , is relatively small over much of the range in  $\psi$ . Additionally, once fully deployed, the system must bear steady loads (such as the vehicle weight) without consuming actuator power. Therefore, for large  $\gamma$  we seek a transmission ratio,  $N$ , that approaches infinity. This

is known as a singular configuration and means that forces imposed on the terrain grippers can be withstood with zero reactive actuator torque. It is also important for robust gripper deployment on rough terrain. Such a configuration, coupled with a carefully engineered path geometry, affords the use of a relatively small motor to lift the vehicle.

The use of a tailored spiral cam geometry is a key contribution of this work and has two core benefits. First, no input actuator power is needed once the mechanism is deployed. Second, the actuator and drive train are shielded from high loads imposed by the terrain, thereby enhancing longevity. The cam and guide pins are still subject to the full external loading. However, we believe these components can be made sturdy without adding substantial mass.

Design of the spiral cam begins with selection of a suitable path geometry (see Fig. 4). The choice need not be limited to a circle, and a variety of curvilinear geometries may be utilized to elicit the desired performance. In general, it is desirable that the terrain grippers collectively behave like a continuous wheel. Therefore, we wish to maximize the number of grippers. Noting that each gripper's guide pin and cam-slot must fully react any axial loading through the gripper, an upper limit on gripper count is imposed for reasons of structural integrity. In our case, a maximum of 7 grippers could be safely utilized.

Two potential drawbacks are inherent to the approach described. Maximizing the number of grippers increases mechanism complexity and potentially reduces robustness. Secondly, the controllable aspect of the overall design introduces unique failure modes. Notably, acute material accumulation between any gripper and the mechanism hub can prevent retraction of the gripper. Additional considerations to prevent such accumulation (i.e., an expandable mesh) may be warranted in some use cases.

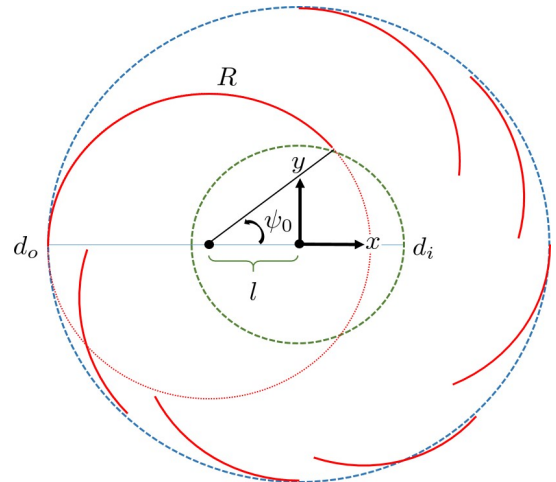


Fig. 5. Selection of spiral geometry (red line) depends on inner diameter (green-dashed line) and outer diameter (blue-dashed line) constraints. The spiral center offset,  $l$ , and permissible spiral radii,  $R$ , are thereby constrained. Note that all but one spiral path are visually truncated to improve readability.

Definition of the number of grippers thereby defines the number of slots that must be cut into the spiral cam. To most effectively utilize space, it was desirable to place the cam on

the interior of the mechanism, within the wheel recess. The recess constrains the outer diameter of the cam to a maximum given by  $d_o$ . An inner diameter constraint,  $d_i$ , must also be imposed on the circle intersecting the slots' starting points (at  $\psi_0$ ). This constraint is based on the diameter of the terrain gripper's guide shaft and is a function of the anticipated loads imposed on the vehicle during operation.

The circular slot naturally stems from  $d_i$  and  $d_o$ , as illustrated in Fig. 5. A natural advantage is that the angle defining the spiral cam transmission ratio,  $\theta$ , can be designed to gradually reach zero at the end of the path. If the path center is offset only in  $x$  or  $y$  (but not both), the path becomes tangential to a circle connecting the path ends when  $\psi = 180^\circ$ . This is true as long as the offset,  $l$ , satisfies Eq. (8). Selecting an offset fixes the slot radius,  $R$ . Alternatively, one may first select  $R$  per Eq. (9), whereby  $l$  is fixed. Fig. 4 provides a visual of these constraints. Note the relationship between offset and slot radius: at maximum offset, the slot radius is minimized. Conversely, radius is maximal at the minimum offset.

$$\frac{d_o - d_i}{4} \leq l \leq \frac{d_o + d_i}{4} \quad (8)$$

$$\frac{d_o - d_i}{4} \leq R \leq \frac{d_o + d_i}{4} \quad (9)$$

As can be seen in Fig. 6, the transmission ratio designed with these criteria produces the desired qualities. Along the majority of the circular slot, the transmission ratio remains low to enable relatively rapid gripper movement. At the end of the movement, the transmission ratio approaches infinity. In order to tune the shape of the transmission ratio curve, the parameters  $R$  or  $l$  may be altered within the confines of Eqs. (8) and (9). If more freedom is required,  $d_i$  may be increased above the minimum imposed by the guide shafts, but may not exceed  $d_o$ .

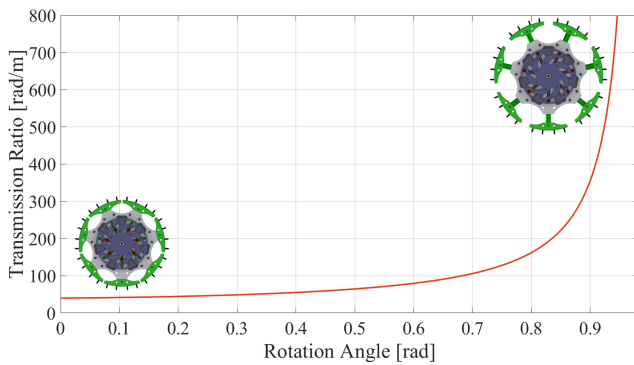


Fig. 6. Spiral cam transmission ratio showing end-of-path singular behavior.

Further flexibility in curve shaping is afforded by relaxing the offset constraints such that both  $x_c$  and  $y_c$  can be nonzero. One may also reduce the number of terrain grippers such that the cam slots span increasingly greater angles; doing so develops higher transmission ratios earlier in the path. If this is still insufficient, one may explore other curvilinear paths like the Archimedes spiral.

#### IV. ELECTROMECHANICAL PROTOTYPE

Based on the analysis in Section III, we created two remotely actuated spiral-cam adaptive wheel prototypes for use with the Georgia Tech AutoRally vehicle. Each prototype features wireless communication and battery power, enabling easy mounting to vehicle wheels without additional wiring. The following section describes the electromechanical design, fabrication, and testing of both the subsystems as well as the fully integrated adaptive AutoRally vehicle.

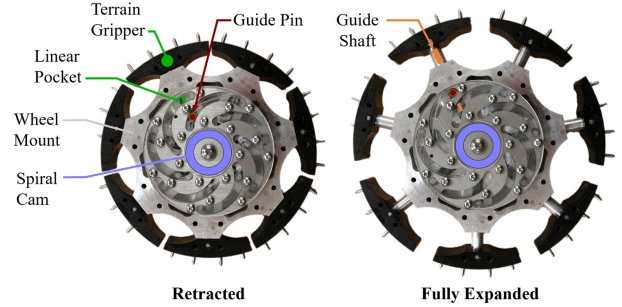


Fig. 7. Annotated view of the mechanism prototype in its retracted and extended states.

##### A. Spiral Cam and Wheel Mount

A photograph of the prototype is shown in Fig. 7. The adaptive wheel system can be conceptualized as beginning with the wheel mount, which attaches rigidly to the wheel. For most kinematic and static analysis, the wheel mount may be considered as fixed. A pair of continuous-motion, Hitec HS-7245MH servo motors controls deployment for each wheel mounted system. To amplify torque, a worm gear is used to provide a 20:1 reduction between the motors' combined output and the spiral cam. A central drive shaft transfers power from the output worm gear to the spiral cam and is rigidly mounted to both components. The spiral cam is thereby constrained axially and radially and rotates concentrically relative to the wheel mount (and the wheel).

The spiral cam utilizes the geometry described in Section III-B. Guide pins ride within the spiral cam slots via bronze bushings. The hardened steel guide pins connect the spiral cam slots to the terrain grippers. The components for the spiral cam and wheel mount were fabricated using CNC and EDM systems.

##### B. Terrain Gripper

Each terrain gripper interfaces with the spiral cam via its guide pin and shaft. The guide shaft links the gripper base to the guide pin. A ball bearing is pressed onto the end of each guide pin. Each ball bearing rides within a different wheel mount linear pocket. As the ball bearing moves within the linear pocket, the terrain gripper displaces radially relative to the wheel mount center.

On the outer face of the gripper is an annular section with a series of blind holes machined into its surface. To create a high friction surface, different devices can be mounted to these blind holes. In this work, we utilize sharpened steel dowel pins. The hardened steel dowel pins are affixed to each blind hole and held in place with a pressed-on plastic sleeve. Before installation, the pins are sharpened to a point and are intended to remain sharp during operation of the mechanism.

### C. Electronics and Control

The adaptive wheel system is designed for wireless control and independent power. A photograph of the electromechanical components is provided in Fig. 8. A sealed recess within each wheel hub is located on the side opposite the spiral cam. This recess contains the control electronics and consists of a lithium-polymer (Lipo) battery (2S, 750 mAh), a microcontroller unit (MCU), two motor drivers, a Hall effect sensor, and an Xbee radio. Note that two motors simultaneously drive the worm and gear, the latter of which is centrally located in Fig. 8. The gear then rotates with the spiral cam shown in Fig. 7 through a central connecting shaft.

Each adaptive wheel system is controlled using wireless signals sent to the Xbee radio transceiver. We utilize a simple bang-bang control scheme where the motor is either commanded full forward, full reverse, or held at stop. Due to this control scheme, efforts were not made to directly minimize gear backlash. The Hall effect sensor is installed into the hub and senses magnets affixed to one of the mechanism's guide shafts. Feedback from the Hall effect sensor is used to terminate motion at either end of travel. For reference, mechanism state changes occur in roughly 2 seconds and draw roughly 1 amp. When the motor is not utilized, the system draws roughly 50 mA. While endurance depends on use scenarios, if the system is switching continuously, each wheel can, in theory, change state up to 1240 times before a battery recharge is needed.

The system has been designed for an IP68 rating. This enables full liquid submersion. The mechanism cap achieves this with an O-ring during attachment to the hub. All other ports in the mechanism are either potted or have their own O-ring for sealing. In total, each mechanism adds approximately 1.18 kg to a wheel. In relation to the standard GT AutoRally vehicle, this represents a mass increase of approximately 11%. We anticipate that this weight penalty can be reduced through more thorough optimization of geometry, material selection, and manufacturing methods.

## V. PERFORMANCE QUANTIFICATION

### A. Terrain Gripper Testing

To quantify the performance of the terrain grippers relative to the original tire, we conducted a series of static friction tests using a simple test cart. These tests measured the force at the onset of motion. Four terrain grippers were attached to the base of the cart. The cart was then positioned on a flat section of terrain, loaded with weight, and pulled with a precision spring force gauge. Once motion began the experiment was stopped. The peak force was verified via video analysis and recorded

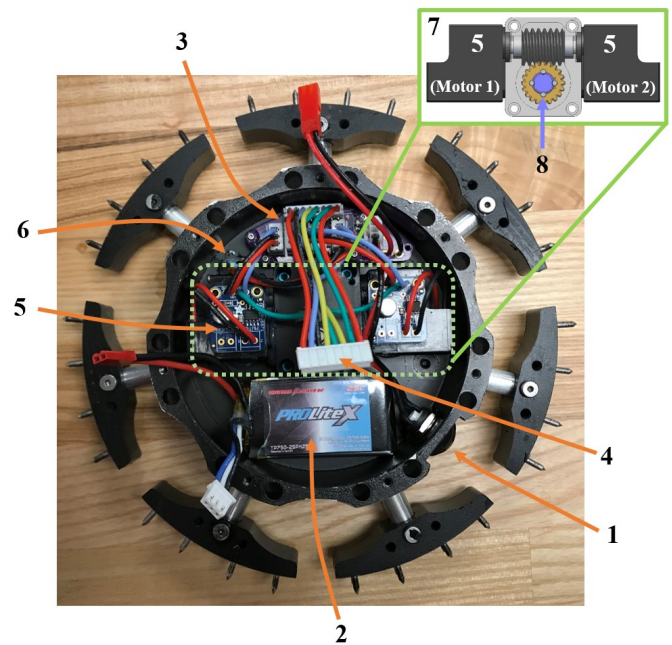


Fig. 8. Annotated on-board electronics and control photo: 1. Power switch, 2. 750 mAh, 2S Lipo, 3. Wheel-mount motherboard, 4. Connection to MCU motherboard, 5. Hitec HS-7245MH servo motor and driver, 6. Hall effect sensor, 7. Power train with worm, gear, and motors, 8. Central drive shaft (to spiral cam).

for a set of cart weights. Four experiments were performed for each operating weight. The results are shown in Figs. 9, 10, and 11.

The sharp spike grippers produce significantly more static traction than the rubber tire on all terrains tested. If we apply the distributed AutoRally vehicle weight of 54 N to a linear model of the data, the spike traction relative to the tire is roughly 160% on dry packed dirt, 190% on grass, and 320% on ice. Dynamic friction testing is expected to produce similar trends, albeit at lower absolute friction values.

Blunt spikes were included in these plots to demonstrate the importance of promoting indentation (via a sharp point) in the terrain gripper design. This is illustrated in Fig. 9, where the blunt spike under-performs the tire by 85%. The relatively poor performance of the blunt spikes helps underscore the need for controllable deployment.

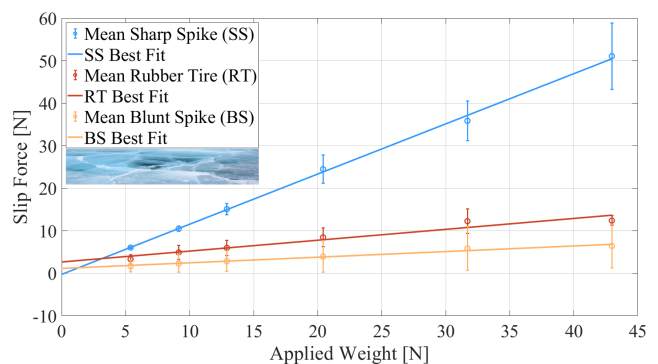


Fig. 9. Slip force versus normal weight for various terrain grippers on ice.

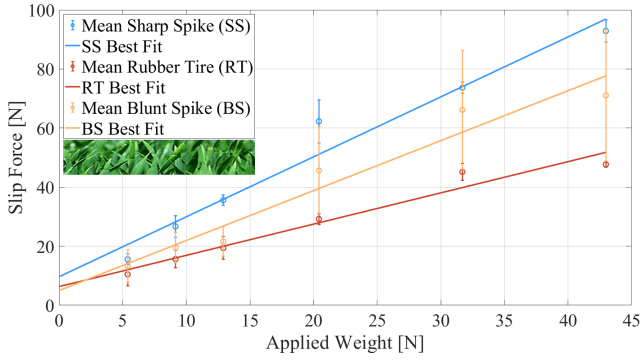


Fig. 10. Slip force versus normal weight for various terrain grippers on grass.

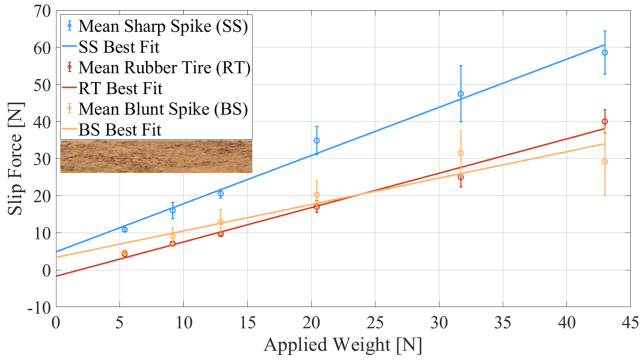


Fig. 11. Slip force versus normal weight for various terrain grippers on dry, packed dirt.

**B. Spiral Cam Transmission Ratio**

Kinematic experiments were performed to order to validate our quantitative spiral cam design methodology. Using a standard 60 fps video recorder, two different, high-visibility paints were applied to the spiral cam and a single gripper. A recording of the mechanism was then taken as the mechanism was hand-actuated. Color tracking software logged the position of each marked component as a function of time. The predicted and measured results are shown in Fig. 12.

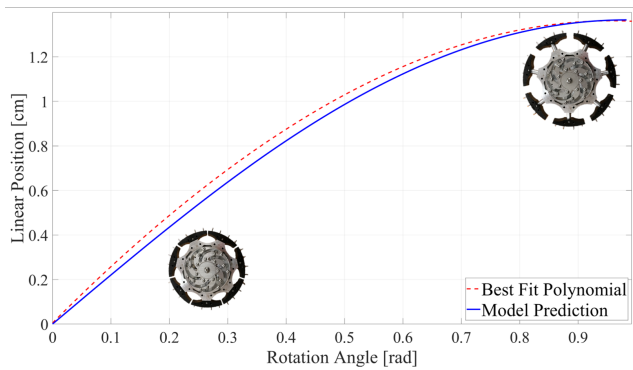


Fig. 12. Modeled spiral cam output versus the measured response.

As can be seen in the figure, the transmission behaves as modeled. Radial velocity of the gripper is greatest at the start of its stroke (from a retracted state) and gradually evolves toward zero at the end of its stroke.

**C. Deployment Testing**

Full system performance was evaluated by installing an adaptive-wheel mechanism on each of the rear (driving) wheels of the Georgia Tech AutoRally platform [5]. The AutoRally platform consists of a modified HPI Baja 5SC 1:5 scale rally car and an onboard computing and sensing system. The system weighs 220 N and has a top speed of 90 km/h. The car uses a rear-wheel drive system actuated by a 10-hp electric motor that is powered by a pair of 4S, 14.8 V lithium-polymer batteries connected in series. For full details on the AutoRally platform, we refer the reader to [5]. The experiments are illustrated in the accompanying video.

Based on the terrain gripper traction results, we chose to examine the performance of sharpened spikes on ice and dirt. To simulate ice, PolyGlide synthetic ice sheets were rigidly fastened to a 1.25 m × 2.5 m wooden platform. The synthetic ice covered all but the platform edges. The platform was then anchored into the ground. The synthetic ice was also wetted with water before each trial to simulate the effect of water bleed on natural ice.

An acceleration test was used to quantify performance. Ice trials began with the vehicle positioned at one end of the platform. A step input command was sent to the motor controller on-board the vehicle. Each trial concluded once the front tires reached the edge of the platform, constituting a total distance of approximately 1.5 meters. Dirt trials were conducted similarly but on a dirt track instead.

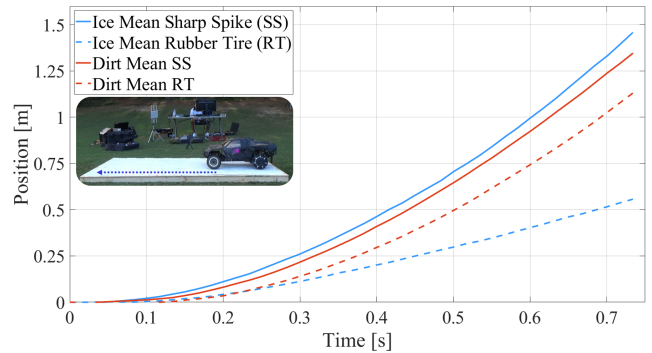


Fig. 13. Synthetic ice and dirt trial results with and without grippers deployed on the Georgia Tech Rally Car.

All trials were conducted with the mechanism installed and with a step input command set to 70% of full throttle. The baseline case held the terrain grippers retracted so that only the rubber tires made contact with the terrain. Test trials were then conducted with the grippers extended. Video analysis was used to determine the kinematics of the vehicle during each trial, from which the results shown in Fig. 13 were obtained. Video was recorded at 60 fps with a wide lens angle mounted perpendicular to vehicle motion (also shown in Fig. 13). Two trials were conducted for each terrain/configuration.

From the position profiles shown in Fig. 13, the advantage of the terrain gripper is evident. When an acceleration coefficient is fitted to the data, the resulting value is 171% greater on ice and 14% greater on dirt with the grippers engaged than with the original rubber tire. The modest gain on dirt is attributed

to unusually good rubber traction on the clay-heavy trial dirt. Performance in grass is expected to follow similar trends. To maximize performance with spikes, updates to the car controller are required. Specifically, throttle values approaching 100% are of interest. Maximizing adaptive performance with control is an area for further study.

While the initial studies have focused on acceleration performance, turning and stopping can also be affected by the adaptive mechanism. If the vehicle does not slip during a turn, we anticipate no degradation in turning behavior. However, at sufficient speeds, increased friction from deployed spikes may impact behavior. This can be positive (reducing lateral slip) or negative (tipping of vehicle). We also anticipate that the deployed terrain grippers will improve stopping performance when brakes are used. The current AutoRally platform does not utilize brakes.

## VI. CONCLUSION

In this paper, we presented a novel system for actively modulating vehicle traction. We formulated functional requirements for adaptive friction modulation and presented a unique spiral cam approach. We analyzed the geometry of the spiral cam and illustrated how a compact rotary-linear transmission could be created. We also showed how a singular configuration can be utilized to minimize power consumption and enhance robustness. We used bench level experiments to illustrate friction improvements as well as the transmission behavior. Finally, we created two prototypes, integrated them into a scale vehicle, and demonstrated how friction modulation can greatly improve performance on a challenging surface (artificial ice).

Our system was designed to be modular yet robust. In its current configuration, the spikes can rather easily deform or tear out of the terrain gripper. This is a result of our attempts to make the design modular, and we are developing methods for more permanent, robust installations.

We believe this approach holds promise for unmanned ground vehicles that must drive aggressively on a range of surfaces. We are excited to combine these techniques with ground property estimation and adaptive control in order to greatly enhance autonomous driving performance.

## ACKNOWLEDGMENT

The authors would like thank to J. Goodwin and N. Tranakiev for their help during testing and validation.

## REFERENCES

- [1] E. Velenis, P. Tsiotras, and J. Lu, "Aggressive maneuvers on loose surfaces: Data analysis and input parametrization," in *2007 Mediterranean Conference on Control & Automation*. IEEE, 2007, pp. 1–6.
- [2] G. W. Burkett, S. A. Velinsky *et al.*, "Evaluation of devices for improving traction control in winter conditions," California. Department of Transportation, Tech. Rep. CA16-2732, 2016.
- [3] R. R. Scheibe, P. M. Engineer, and K. C. Kirkland, "An overview of studded and studless tire traction and safety," Washington State Department of Transportation, Tech. Rep. WA-RD 551.1, 2002.
- [4] G. Skouvaklis, J. R. Blackford, and V. Koutsos, "Friction of rubber on ice: A new machine, influence of rubber properties and sliding parameters," *Tribology International*, vol. 49, pp. 44–52, 2012.
- [5] B. Goldfain, P. Drews, C. You, M. Barulic, O. Velez, P. Tsiotras, and J. M. Rehg, "Autorially: An open platform for aggressive autonomous driving," *IEEE Control Systems Magazine*, vol. 39, no. 1, pp. 26–55, 2019.
- [6] T. Aoki, Y. Murayama, and S. Hirose, "Development of a transformable three-wheeled lunar rover: Tri-star iv," *Journal of Field Robotics*, vol. 31, no. 1, pp. 206–223, 2014.
- [7] C. Grand, P. Bidaud, and N. Jarrassé, "Innovative concept of unfoldable wheel with an active contact adaptation mechanism," in *12th IFToMM World Congress. Besancon*. Citeseer, 2007, pp. 3890–3895.
- [8] Y.-S. Kim, G.-P. Jung, H. Kim, K.-J. Cho, and C.-N. Chu, "Wheel transformer: A miniaturized terrain adaptive robot with passively transformed wheels," in *2013 IEEE International Conference on Robotics and Automation*. IEEE, 2013, pp. 5625–5630.
- [9] J. Park, D. H. Kong, and H.-W. Park, "Design of anti-skid foot with passive slip detection mechanism for conditional utilization of heterogeneous foot pads," *IEEE Robotics and Automation Letters*, vol. 4, no. 2, pp. 1170–1177, 2019.
- [10] A. T. Asbeck, S. Kim, M. R. Cutkosky, W. R. Provancher, and M. Lanzetta, "Scaling hard vertical surfaces with compliant microspine arrays," *The International Journal of Robotics Research*, vol. 25, no. 12, pp. 1165–1179, 2006.
- [11] K. Carpenter, N. Wiltsie, and A. Parness, "Rotary microspine rough surface mobility," *IEEE/ASME Transactions on Mechatronics*, vol. 21, no. 5, pp. 2378–2390, 2015.
- [12] D.-Y. Lee, S.-R. Kim, J.-S. Kim, J.-J. Park, and K.-J. Cho, "Origami wheel transformer: A variable-diameter wheel drive robot using an origami structure," *Soft robotics*, vol. 4, no. 2, pp. 163–180, 2017.
- [13] T. G. Nelson, T. K. Zimmerman, S. P. Magleby, R. J. Lang, and L. L. Howell, "Developable mechanisms on developable surfaces," *Science Robotics*, vol. 4, no. 27, 2019.
- [14] K. Nagatani, M. Kuze, and K. Yoshida, "Development of transformable mobile robot with mechanism of variable wheel diameter," *J. Robot. Mechatron*, vol. 19, pp. 252–253, 2007.
- [15] S. Hirose, E. F. Fukushima, R. Damoto, and H. Nakamoto, "Design of terrain adaptive versatile crawler vehicle helios-vi," in *Proceedings 2001 IEEE/RSJ International Conference on Intelligent Robots and Systems. Expanding the Societal Role of Robotics in the Next Millennium (Cat. No. 01CH37180)*, vol. 3. IEEE, 2001, pp. 1540–1545.
- [16] S.-C. Chen, K.-J. Huang, W.-H. Chen, S.-Y. Shen, C.-H. Li, and P.-C. Lin, "Quattroped: a leg-wheel transformable robot," *IEEE/ASME Transactions On Mechatronics*, vol. 19, no. 2, pp. 730–742, 2013.
- [17] Y. She, C. J. Hurd, and H.-J. Su, "A transformable wheel robot with a passive leg," in *2015 IEEE/RSJ International Conference on Intelligent Robots and Systems (IROS)*. IEEE, 2015, pp. 4165–4170.
- [18] B. Spice, "Researchers reinventing the wheel for vehicles of the future - news - carnegie mellon university," Oct 2018. [Online]. Available: <https://www.cmu.edu/news/stories/archives/2018/october/reinventing-wheel.html>
- [19] Z. Li, S. Ma, B. Li, M. Wang, and Y. Wang, "Design and basic experiments of a transformable wheel-track robot with self-adaptive mobile mechanism," in *2010 IEEE/RSJ International Conference on Intelligent Robots and Systems*. IEEE, 2010, pp. 1334–1339.
- [20] F. Michaud, D. Letourneau, M. Arsenault, Y. Bergeron, R. Cadrin, F. Gagnon, M.-A. Legault, M. Millette, J.-F. Paré, M.-C. Tremblay *et al.*, "Multi-modal locomotion robotic platform using leg-track-wheel articulations," *Autonomous Robots*, vol. 18, no. 2, pp. 137–156, 2005.
- [21] A. K. Leichman, "Traction invention conquers ice, snow, sand, mud," Jan 2013. [Online]. Available: <https://www.israel21c.org/traction-invention-conquers-ice-snow-sand-mud/>
- [22] N. Fukuoka, "Advanced technology of the studless snow tire," *JSAE review*, vol. 15, no. 1, pp. 59–66, 1994.
- [23] M. Al-Assi and E. Kassem, "Evaluation of adhesion and hysteresis friction of rubber-pavement system," *Applied Sciences*, vol. 7, no. 10, p. 1029, 2017.
- [24] S. Ella, P.-Y. Formagne, V. Koutsos, and J. R. Blackford, "Investigation of rubber friction on snow for tyres," *Tribology International*, vol. 59, pp. 292–301, 2013.
- [25] B. N. Persson, U. Tartaglino, O. Albohr, and E. Tosatti, "Rubber friction on wet and dry road surfaces: The sealing effect," *Physical review B*, vol. 71, no. 3, p. 035428, 2005.